

Video Article

Characterizing Lewis Pairs Using Titration Coupled with In Situ Infrared Spectroscopy

Carly S. Hanson¹, James J. Devery¹¹Department of Chemistry & Biochemistry, Loyola University ChicagoCorrespondence to: James J. Devery at jdevery@luc.eduURL: <https://www.jove.com/video/60745>DOI: [doi:10.3791/60745](https://doi.org/10.3791/60745)

Keywords: Chemistry, Issue 156, chemistry, infrared spectroscopy, Lewis acid, Lewis base, carbonyl, titration

Date Published: 2/20/2020

Citation: Hanson, C.S., Devery, J.J. Characterizing Lewis Pairs Using Titration Coupled with In Situ Infrared Spectroscopy. *J. Vis. Exp.* (156), e60745, doi:10.3791/60745 (2020).

Abstract

Lewis acid-activation of carbonyl-containing substrates is a fundamental basis for facilitating transformations in organic chemistry. Historically, characterization of these interactions has been limited to models equivalent to stoichiometric reactions. Here, we report a method utilizing in situ infrared spectroscopy to probe the solution interactions between Lewis acids and carbonyls under synthetically relevant conditions. Using this method, we were able to identify 1:1 complexation between GaCl₃ and acetone and a highly ligated complex for FeCl₃ and acetone. The impact of this technique on mechanistic understanding is illustrated by application to the mechanism of Lewis acid-mediated carbonyl-olefin metathesis in which we were able to observe competitive binding interactions between substrate carbonyl and product carbonyl with the catalyst.

Video Link

The video component of this article can be found at <https://www.jove.com/video/60745/>

Introduction

The utilization of Lewis acids to activate substrates containing carbonyls is ubiquitous in organic synthetic methods^{1,2,3,4}. The study of these interactions has relied on solid state X-ray crystallography, as well as in situ NMR spectroscopy². Limitations of these techniques manifest from artifacts that arise from crystallization, or the inability to probe paramagnetic Lewis acids via NMR analysis. To overcome these issues, chemists have employed infrared (IR) spectroscopy to determine the exact structure of Lewis pairs. Further, IR has been utilized to determine Lewis acidity^{4,5,6,7,8,9}. The Susz lab studied the solid-state interactions of Lewis acids and carbonyls in the stoichiometric regime. Utilizing IR in conjunction with elemental analysis, the Susz group was able to elucidate the structures of neat, 1:1 mixtures of Lewis pairs. This analysis provided a great deal of insight into structural ramifications of the interactions of simple carbonyl compounds with commonly utilized Lewis acids in the solid state, and of particular interest to our lab: FeCl₃^{10,11}. We posited that we could add to the existing understanding of the interactions of these important Lewis pairs via an in situ method that examines synthetically relevant conditions.

In situ IR enables chemists to perform real-time measurements of functional group conversions in situ. These data supply key insights into reaction rates to support hypotheses about the operating mechanisms of a process and to influence of reaction performance. Real-time observations allow chemists to directly track the interconversion of reaction components over the course of the reaction, and the information gleaned can be employed by the synthetic chemist in the development of new compounds and the optimization of synthetic routes and new chemical processes.

Employing in situ IR spectroscopy as a detection method, we probed the substrates and intermediates that participate in the catalytic cycle of metal-mediated carbonyl-olefin metathesis¹². The Fe(III)-catalyzed carbonyl-olefin metathesis process, developed by the Schindler lab, exemplifies a powerful method for the production of C=C bonds from functional groups utilized ubiquitously in the construction of complex molecules^{13,14,15}. Since the original report, this process has inspired a plethora of synthetic developments beyond the utilization of Fe(III)^{16,17,18,19,20,21,22,23,24,25}. Importantly, this reaction requires that the Lewis acid catalyst differentiate between a substrate carbonyl and a product carbonyl for successful reactivity. To observe this competitive interaction under synthetically relevant conditions, we combined titration with the continuous observation provided by in situ IR.

We believe this method is of general importance to chemists studying carbonyl-centered reactions catalyzed by Lewis acids. This detailed demonstration aims to help chemists apply this technique to their system of study.

Protocol

1. Open-air reference spectrum

1. Open the data acquisition software. Click **Instrument**. Under the **Configure** tab, click **Collect Background**. Click **Continue**. Set scans to **256** and click **OK** to collect a background.
NOTE: Make sure the probe is in the same position in which data collection will take place. Position changes of the probe may impact spectra.

2. Solvent reference spectrum

1. In the data acquisition software, click **File**. Click **New**. Click **QuickStart**.
2. Set **Duration** to 15 min and **Sample Interval** to 15 s. Click **Create** to create experiment.
NOTE: At this point, the chemical system must be attached to the in situ IR probe to proceed. The following steps are for the preparation of the chemical system to be studied.
3. Under inert atmosphere, add Lewis acid to a flame-dried 25 mL 2-neck round bottom flask charged with a stir bar (**Figure 1B**). Seal the flask with rubber septa and attach an Ar-filled balloon to the flask. Add desired volume of anhydrous solvent via syringe (minimum 3 mL) (**Figure 1C**).
NOTE: FeCl_3 is not soluble in dichloroethane (DCE). GaCl_3 is soluble in DCE.
4. Remove one septum and attach the flask to the in situ IR probe (**Figure 1D**). Place the flask in a temperature-controlled bath set to desired temperature (**Figure 1E**).
5. Start the experiment in the data acquisition software by clicking the ► button to begin collecting data, and stop collecting data after 2 min.
NOTE: The name of this file is the solvent reference spectrum that you will use in step 3.1.3.

3. Titration software setup

1. Creating new titration experiment
 1. In the data acquisition software, click **File | New | Quick Start**. Set **Duration** to 8 h and **Sample Interval** to 15 s.
NOTE: The data acquisition has the ability to set experiment duration between 15 min and 2 d and sample interval between 15 s and 1 h.
 2. Click **Create** to create experiment. In the data acquisition software, go to **Spectra** tab and click **Add Spectra**. Click **From File** and open appropriate solvent reference spectrum obtained in step 2. Check the box with the time signature. Click **OK**.
 3. Start experiment in the data acquisition software by clicking the ► button to begin collecting data.
2. Click **Solvent Subtraction** and select appropriate reference spectrum added in step 3.1.3. Stir for 15 min to reach temperature. Use the in situ IR probe to determine temperature.

4. Titration procedure

1. Add 10 μL of carbonyl analyte via syringe (**Figure 1F**).
2. Observe signal response on the data acquisition (**Figure 2**). System will shift from equilibrium and change with time.
3. When the IR signal stabilizes and remains constant, collect IR spectrum.
NOTE: The data acquisition collects spectra at a set frequency. Data in our lab are collected every 15 s. We note the time at which the system reaches equilibrium and use the spectrum collected at the time for analysis.
4. Repeat steps 4.1-4.3 until desired amount of analyte is added.
NOTE: FeCl_3 mixture becomes homogeneous once 1 equiv **1** is added and GaCl_3 mixture remains homogeneous regardless of amount of **1** added.

5. Analysis of IR spectra

1. Export data for the data acquisition software.
 1. Click **File | Export | Multi-spectrum file**.
 2. Under **Format**, check **CSV** and under **Data**, check **Raw**. Click **Export** to export IR data to spreadsheet or mathematical processing software.
2. Plot desired region of IR spectrum, as shown in **Figure 3A,D**.
3. Examine the spectrum for transitions and/or isosbestic points.
4. Separate spectra by progression, as shown in **Figure 3B,C** for GaCl_3 and **Figure 3E,F** for FeCl_3 .

6. Component analysis

1. Identify λ_{max} of each species of interest, as shown in **Figure 4A** for GaCl_3 and **1** and **Figure 4D** for FeCl_3 and **1**, to generate a table of Absorbance vs. equivalent of analyte added, as shown in **Figure 4B** for GaCl_3 and **Figure 4E** for FeCl_3 .

- To account for dilution, multiply the absorbance by the total volume of the solution for each spectrum, as shown in **Figure 4B** for GaCl₃ and **Figure 4E** for FeCl₃.
- Plot product of absorbance*volume as a function of equivalents of analyte, as shown in **Figure 4C** for GaCl₃ and **Figure 4F** for FeCl₃.

7. Analysis of consumption of species

- For in situ-generated species that can be identified, plot a Beer-Lambert relationship, as shown in **Figure 5A**.
- For known species, measure the impact of concentration on Absorbance at the desired λ_{max} and plot a Beer-Lambert relationship.
- Using the two Beer-Lambert relationships, determine the observed in situ amounts of the species of interest, as shown in **Figure 5B**.
NOTE: $C_{\text{MAX}} = 2$ mmol as defined by the amount of FeCl₃ present. C_{ADD} is the moles of acetone (**1**) added. C_{COORD} is the moles of FeCl₃-acetone complex (**3**). C_{OBS} is the moles of unbound **1**. C_{ND} is the moles of **1** not detected. $C_{\text{MAX}} - C_{\text{COORD}}$ is the moles of **3** that have been consumed.
- Plot C_{ND} vs. $(C_{\text{MAX}} - C_{\text{COORD}})$ to determine if there is a correlation, as shown in **Figure 5C**.
NOTE: The slope of this line will be in moles of species **1** per moles of species **3**.

Representative Results

In this study, in situ IR-monitored titration was used to observe the interactions of **1** and GaCl₃ as well as **1** and FeCl₃ (**Figure 6**)¹². Using this collection of protocols, we were able to determine that GaCl₃ and **1** form 1:1 complex **2** in solution. Alternatively, when FeCl₃ and **1** are combined, more complex behavior is observed. **Figure 6** displays the equilibria we were examining. **Figure 1** displays the physical setup of the titration of FeCl₃ with **1**. **Figure 2** displays the raw feed of data obtained by the in situ IR using the data acquisition software for the titration of FeCl₃ with **1**. **Figure 3** displays the process of extracting the transitions that result from this titration method applied to GaCl₃ and FeCl₃. **Figure 4** displays the extraction of λ_{max} data of the titration of GaCl₃ with **1** and the titration of FeCl₃ with **1**. **Figure 5** displays the extraction of complex coordination behavior from the titration of FeCl₃ with **1**. **Figure 7** displays an application of these protocols for the examination of competitive access to a Lewis acid. **Figure 8** shows the application of these protocols to revising the mechanism of metal catalyzed carbonyl-olefin metathesis.

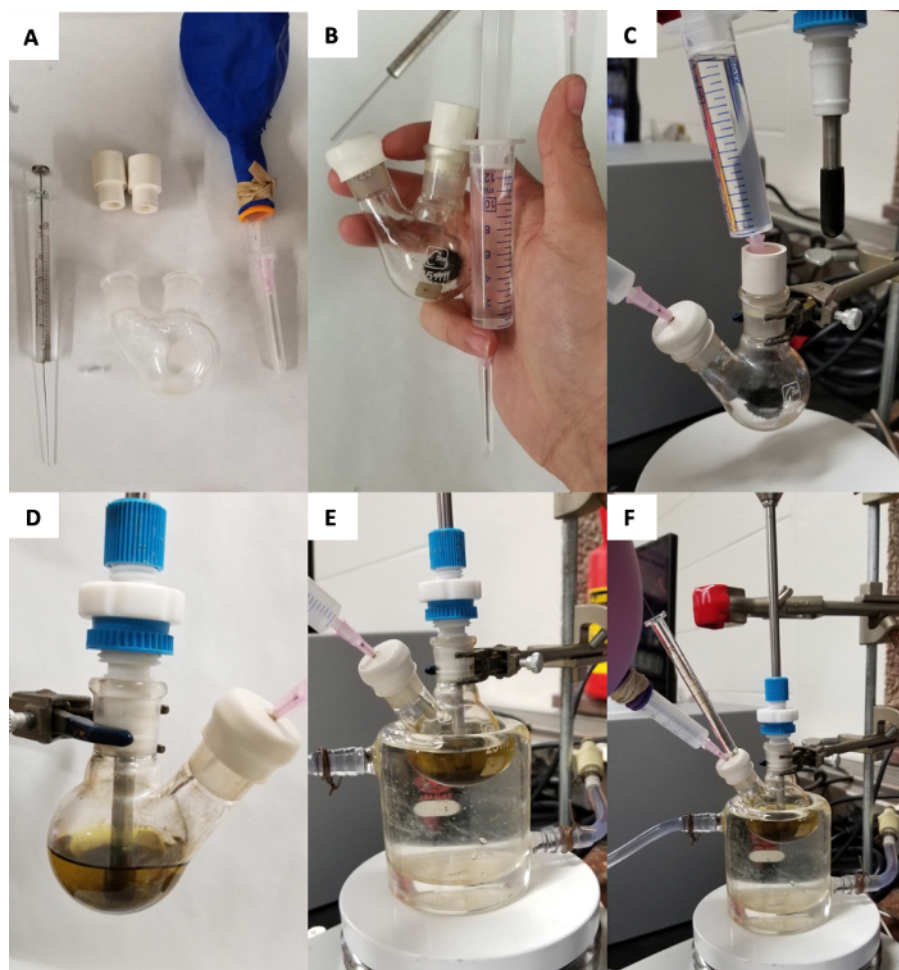


Figure 1: Visual guide to system setup. Necessary components for performing the titration (A). Assembled components prior to attachment to the in situ IR (B). Flask with Ar and ready for solvent addition (C). Flask attached to the in situ IR with solvent (D). Flask under temperature control (E). Ready for addition of analyte (F). [Please click here to view a larger version of this figure.](#)

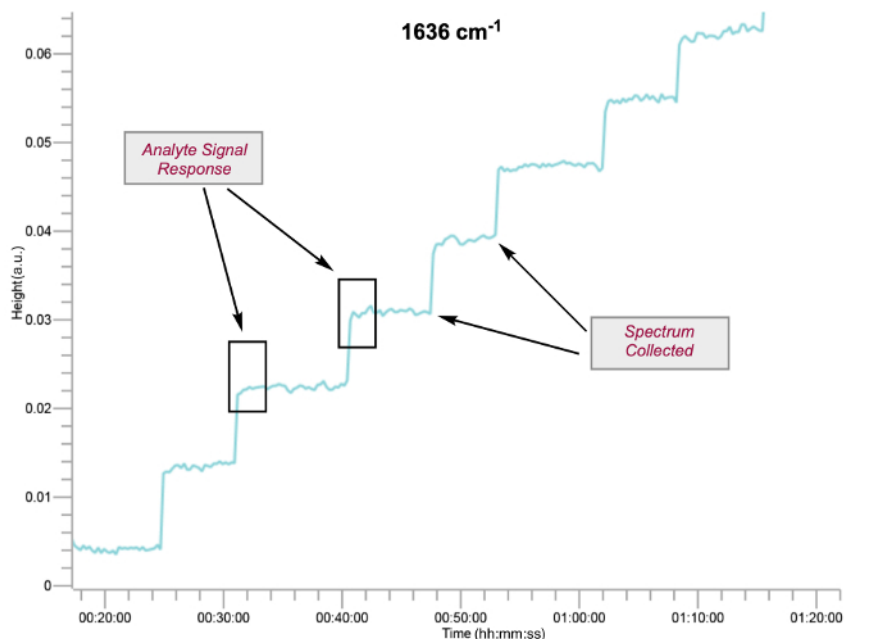


Figure 2: Analyte signal response in the data acquisition interface at 1636 cm⁻¹ for titration of 2 mmol FeCl₃ in 12 mL of DCE with 1. The spectrum is collected when the system is at equilibrium, after analyte addition. [Please click here to view a larger version of this figure.](#)

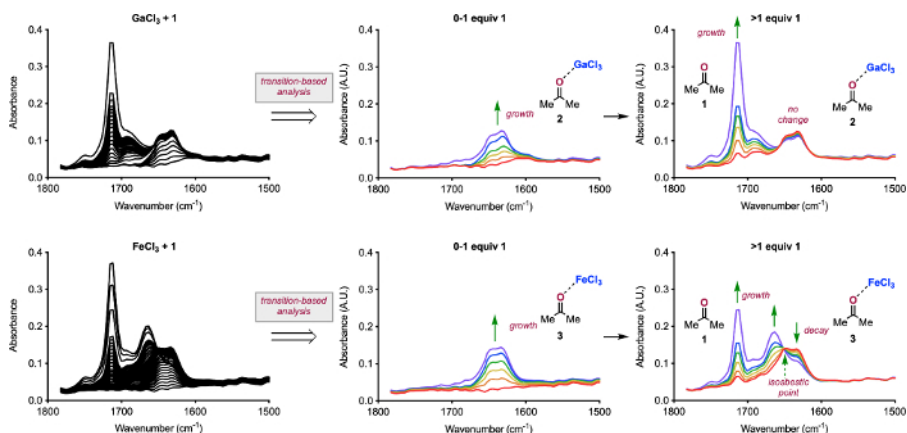


Figure 3: Analysis of IR spectra. Spectra collected for the titrations GaCl₃ with 0-4 equiv 1 (A) and FeCl₃ with 0-4 equiv 1 (D). Breakdown of titration of GaCl₃ with 0-1 equiv 1 showing the formation of 2 (B) and with 1-4 equiv 1 showing the presence of 1 (C). Breakdown of titration of FeCl₃ with 0-1 equiv 1 showing the formation of 3 (E) and with 1-4 equiv 1 showing the presence of 1, the consumption of 3, and the formation of a new species (F). Reprinted (adapted) with permission from Hanson, C. S., et al¹². Copyright 2019 American Chemical Society. [Please click here to view a larger version of this figure.](#)

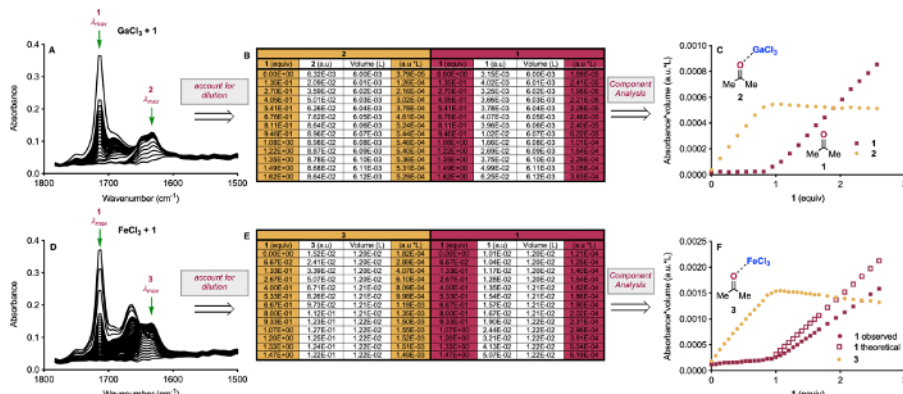


Figure 4: Extraction of λ_{max} data from IR for Component Analysis. Spectra collected for the titrations GaCl_3 with 0–4 equiv **1** with the λ_{max} for **1** and **2** indicated (A) and FeCl_3 with 0–4 equiv **1** with the λ_{max} for **1** and **3** indicated (D). Table showing representative data normalized to account for dilution for GaCl_3 (B) and for FeCl_3 (E). Data from (B) plotted for component analysis of titration of GaCl_3 with **1** (C) and for component analysis of titration of FeCl_3 with **1** (F). Reprinted (adapted) with permission from Hanson, C. S., et al¹². Copyright 2019 American Chemical Society. [Please click here to view a larger version of this figure.](#)

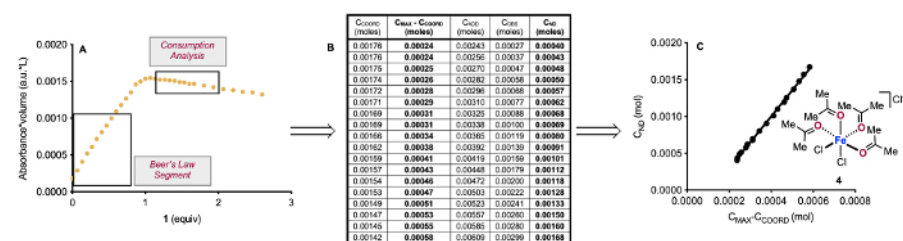


Figure 5: Consumption analysis of titration of FeCl_3 with **1.** Segment of IR data used to generate a Beer-Lambert relationship for **[3]** and the segment of IR data used to determine the consumption of **3** (A). Moles of each **1**-containing species measured by IR (B). Plot of moles of **1** not detected vs. moles of **3** consumed (C). Reprinted (adapted) with permission from Hanson, C. S., et al¹². Copyright 2019 American Chemical Society. [Please click here to view a larger version of this figure.](#)

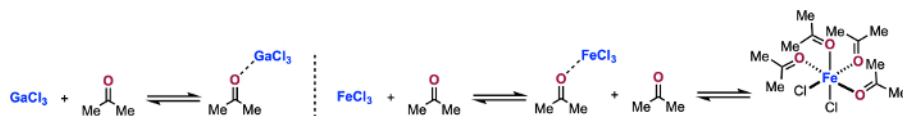


Figure 6: Lewis acid/base equilibria probed in this study. Titrations of GaCl_3 with **1** to form **2** and FeCl_3 with **1** to form **3** and **4** are reported. [Please click here to view a larger version of this figure.](#)

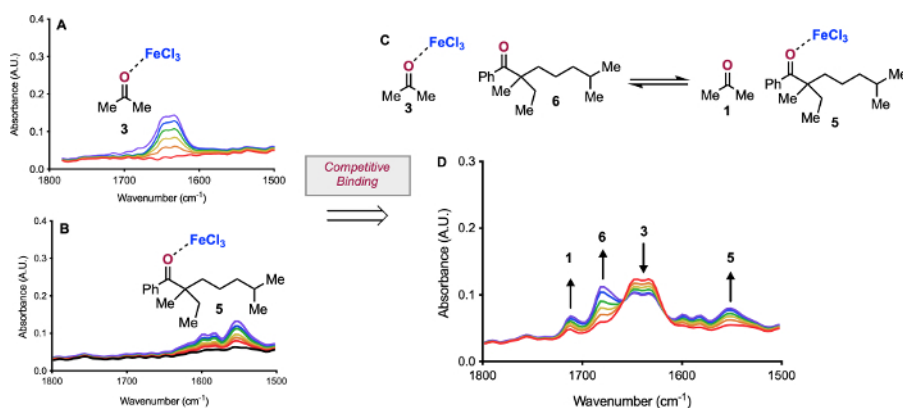


Figure 7: Competitive binding experiment. Carbonyl region of IR spectrum of **3** (A) and of IR spectrum of **5** (B). Equilibrium probed in titration of **3** with **6** (C). IR data of titration of **3** with **1** equiv **6** (D). Reprinted (adapted) with permission from Hanson, C. S., et al¹². Copyright 2019 American Chemical Society. [Please click here to view a larger version of this figure.](#)

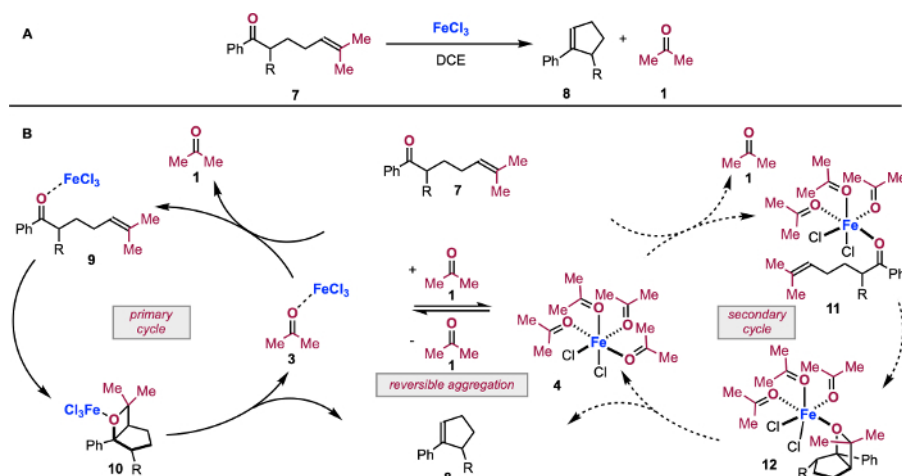


Figure 8: Application of in situ IR data in mechanistic proposal. Carbonyl-olefin metathesis reaction of **7** (A). The revised mechanistic proposal of carbonyl-olefin metathesis facilitated by titration coupled with in situ IR spectroscopy (B). Reprinted (adapted) with permission from Hanson, C. S., et al.¹². Copyright 2019 American Chemical Society. [Please click here to view a larger version of this figure.](#)

Discussion

Under anhydrous conditions, Lewis acids can have a range of solubilities. The two examples we have presented are GaCl₃ and FeCl₃ in DCE. GaCl₃ is homogeneous at the onset of the titration, while FeCl₃ is largely insoluble. Beginning with the homogeneous solution of GaCl₃, we completed a titration from 0-4 equiv **1** in 10 μ L increments and extracted the IR spectra (Figure 3A). Examination of the transitions that occur over the course of the titrations shows a formation of a single species in the carbonyl region at 1630 cm⁻¹, which grows from 0-1 equiv **1** (Figure 3B)^{26,27}. When greater than 1 equiv **1** is added to the solution, no change in the peak at 1630 cm⁻¹ occurs and unbound **1** is observed at 1714 cm⁻¹ (Figure 3C). These results are consistent with the formation of **2**. When the same titration is performed with FeCl₃ (Figure 3D), a peak at 1636 cm⁻¹ forms from 0-1 equiv **1**, which is consistent with **3** (Figure 3E). Importantly, the mixture becomes homogenous once 1 equiv **1** is achieved. When the titration proceeds beyond 1 equiv **1**, unbound **1** is observed at 1714 cm⁻¹, **3** decreases in intensity, an isosbestic point resolves at 1648 cm⁻¹, and a new peak at 1663 cm⁻¹ forms.

Using the titration IR data, the equivalents of analyte used can be employed to perform Component Analysis of the solution interactions (Figure 4). To account for dilution, we can employ a normalization with respect to volume of the Beer-Lambert equation (eq. 1):

$$AV = \epsilon ln \quad (1)$$

where 1) both absorbance (A) and volume (V) are measurable terms; 2) molar absorptivity (ϵ) and pathlength (l) are constant, allowing 3) number of moles (n) to be examined. The normalized absorbance can easily be computed in a spreadsheet (Figure 4B,D), and then this term can be plotted against equivalents of analyte. In Figure 4C, we can see that the signal for **2** increases linearly with respect to 1 until 1 equiv, at which point the signal for **1** increases linearly and **2** is unchanged. In Figure 4F, we see a similar linear increase in the signal of **3** to 1 equiv **1**, followed by the presence of **1** beyond 1 equiv added. However, we also observe a linear decrease in the intensity of **3**, and we observe less **1** than we should, assuming similar behavior to GaCl₃.

Yet more information is available from the IR data for the titration of FeCl₃ with **1**. The maximum amount of **3** that can form is defined by the amount of FeCl₃ added ($C_{MAX} = 2$ mmol FeCl₃ in the example titration). We know the amount of **1** we add to the flask (C_{ADD}), and we can measure the amount of unbound **1** we observe at 1714 cm⁻¹ (C_{OBS}) and the amount of **3** we observe at 1636 cm⁻¹ (C_{COORD}) using Beer-Lambert relationships. Lastly, we know we cannot account for all of the **1** added to the flask as free **1** or **3**, indicating that some **1** is not detected (C_{ND}). We can combine these terms for **1** in the following mass balance (eq. 2):

$$C_{ADD} = C_{OBS} + C_{COORD} + C_{ND} \quad (2)$$

We can use the titration data to calculate the values of these terms in each IR spectrum generated during the titration (Figure 5B). With these values, we can plot the amount of **1** missing (C_{ND}) as a function of the amount **3** consumed ($C_{MAX} - C_{COORD}$) to determine if there is a correlation (Figure 5C). This correlation is consistent with 3 equiv **1** consuming 1 equiv **3**, which may form a complex similar to **4**. We have obtained further support for this number of attached ketones via examination of solution conductivity, which is consistent with one or more of the chlorides being displaced to the outer sphere of Fe(III), and X-ray crystallography of an analogous structure with benzaldehyde¹². However, it is likely that there is a mixture of different types of highly-ligated structures that are formed in solution, as is indicated by our non-whole number slopes in our consumption analysis in Figure 5, and the crystal structure we observe may simply be the one complex that precipitates.

In addition to the interactions between two species, this method can be used to probe competitive interactions (Figure 7). By establishing the formation and spectral properties of **3** (Figure 7A) and **5** (Figure 7B), the competition of carbonyls for access to the Lewis acid can be observed. By preforming **3** in solution, we can examine how **6** displaces **1** (Figure 7C). When we probe this system, we see that as we add **6** to **3**, not all **6** binds to FeCl₃. However, we do observe the consumption of **3** with concomitant presence of **1**, as well as the formation of **5**.

Using this type of competition experiment, we have been able to simulate the state of FeCl₃ as a catalyst in carbonyl-olefin metathesis (Figure 8). We previously demonstrated that at low turnovers, carbonyl-olefin metathesis operates via the primary cycle in Figure 8B²⁶. Substrate **7**

interacts with FeCl_3 to form complex **9** as the resting state of the cycle. Complex **9** then undergoes turnover-limiting [2+2]-cycloaddition to form oxetane complex **10**. Retro-[2+2] yields cycloalkene product **8** and **3**, which in turn must have the molecule of **1** displaced by a molecule of **7**. However, as the [1] increases, **3** is converted to complex **4**. Coordinatively saturated **4** then either sequesters FeCl_3 or is catalytically competent, resulting in a parallel cycle via ketone complex **11** and oxetane complex **12**.

In conclusion, the utilization of in situ IR to monitor the titration of Lewis acids with carbonyl compounds allows chemists to gain insight into Lewis acid/base solution interactions under synthetically relevant conditions. Not only can this technique be employed to identify discrete structures, but it can be employed to observe the transition of one discrete species into another, as well. Findings from this method have been utilized to propose the mechanism of other metathesis reactions²⁹. We are currently using data gathered via this method to facilitate the reactivity of recalcitrant substrates in carbonyl-olefin metathesis, as well as to develop new forms of metathesis reactions. Lastly, the competitive interactions between substrate carbonyls and product carbonyls likely impact other Lewis acid-catalyzed reactions. We are employing this method to examine these other catalytic regimes.

Disclosures

This article was produced with support by Mettler-Toledo Autochem Inc., which is the producer of the instrument utilized in this article.

Acknowledgments

We thank Loyola University Chicago, Merck, Co., Inc., and the NIH/National Institute of General Medical Sciences (GM128126) for financial support. We thank Mettler-Toledo Autochem Inc. for their support in the production of this article.

References

1. NATO ASI Series, Ser. C: Mathematical and Physical Sciences: Selectivities in Lewis Acid Promoted Reactions. **289**, Kluwer, (1989).
2. Santelli, M., Pons, J.M. *Lewis Acids and Selectivity in Organic Synthesis*. CRC Press, (1996).
3. Yamamoto, H., Ed., *Lewis Acids in Organic Synthesis*. Wiley-VCH, (2000).
4. Satchell, D. P. N., Satchell, R. S. Quantitative Aspects of the Lewis Acidity of Covalent Metal Halides and Their Organo Derivatives. *Chemical Reviews*. **69**, 251-278 (1969).
5. Mohammad, A., Satchell, D. P. N., Satchell, R. S. Quantitative Aspects of Lewis Acidity. Part VIII. The Validity of Infrared Carbonyl Shifts as Measures of Lewis Acid Strength. The Interaction of Lewis Acids and Phenalen-1-one(Perinaphthenone). *Journal of the Chemical Society B: Physical Organic*. 723-725 (1967).
6. Satchell, D. P. N., Satchell, R. S. Quantitative Aspects of Lewis Acidity. *Q. Chemical Society Reviews*. **25**, 171-199 (1971).
7. Driessen, W. L., Groeneveld, W. L. Complexes with Ligands Containing the Carbonyl Group. Part I: Complexes with Acetone of Some Divalent Metals Containing Tetrachloro-ferrate(III) and -indate(III) Anions. *Recueil des Travaux Chimiques des Pays-Bas*. **88**, 977-988 (1969).
8. Driessen, W. L., Groeneveld, W. L. Complexes with Ligands Containing the Carbonyl Group. Part III: Metal (II) Acetaldehyde, Propionaldehyde and Benzaldehyde Solvates. *Recueil des Travaux Chimiques des Pays-Bas*. **90**, 87-96 (1971).
9. Driessen, W. L., Groeneveld, W. L. Complexes with Ligands Containing the Carbonyl Group. Part IV Metal(II) Butanone, Acetophenone, and Chloroacetone Solvates. *Recueil des Travaux Chimiques des Pays-Bas*. **90**, 258-264 (1971).
10. Chalandon, P., Susz, B. P. Etude de Composés d'Addition des Acides de Lewis. VI Spectre d'Absorption Infrarouge de l'Acétone-Trifluorure de Bore; Spectre d'Absorption Infrarouge et Moment de Dipôle du Di-propyl-cétone-trifluorure de Bore. *Helvetica Chimica Acta*. **41**, 697-704 (1958).
11. Susz, B. P., Chalandon, P. Etude de Composés d'Addition des Acides de Lewis. IX. - Spectres d'Absorption Infrarouge des Composés Formés par la Benzophénone et l'Acétophénone avec BF_3 , FeCl_3 , ZnCl_2 et AlCl_3 et Nature de la Liaison Oxygène-Métal. *Helvetica Chimica Acta*. **41**, 1332-1341 (1958).
12. Hanson, C. S., Psaltakis, M. C., Cortes, J. J., Devery, J. J., III Catalyst Behavior in Metal-Catalyzed Carbonyl-Olefin Metathesis. *Journal of the American Chemical Society*. **141**, 11870-11880 (2019).
13. Ludwig, J. R., Schindler, C. S. Lewis Acid Catalyzed Carbonyl-Olefin Metathesis. *Synlett*. **139**, 2960 (2017).
14. Becker, M. R., Watson, R. B., Schindler, C. S. Beyond Olefins: New Metathesis Directions for Synthesis. *Chemical Society Reviews*. **47**, 7867-7881 (2018).
15. Riehl, P. S., Schindler, C. S. Lewis Acid-Catalyzed Carbonyl-Olefin Metathesis. *Trends in Analytical Chemistry*. **1**, 272-273 (2019).
16. Ludwig, J. R., Zimmerman, P. M., Gianino, J. B., Schindler, C. S. Iron(III)-Catalyzed Carbonyl-Olefin Metathesis. *Nature*. **533**, 374-379 (2016).
17. Ma, L. et al. FeCl_3 -Catalyzed Ring-Closing Carbonyl-Olefin Metathesis. *Angewandte Chemie International Edition*. **55**, 10410-10413 (2016).
18. McAtee, C. C., Riehl, P. S., Schindler, C. S. Polycyclic Aromatic Hydrocarbons via Iron(III)-Catalyzed Carbonyl-Olefin Metathesis. *Journal of the American Chemical Society*. **139**, 2960-2963 (2017).
19. Groso, E. J. et al. 3-Aryl-2,5-Dihydropyrroles via Catalytic Carbonyl-Olefin Metathesis. *ACS Catalysis*. **8**, 2006-2011 (2018).
20. Ludwig, J. R. et al. Interrupted Carbonyl-Olefin Metathesis via Oxygen Atom Transfer. *Science*. **361**, 1363-1369 (2018).
21. Albright, H. et al. GaCl_3 -Catalyzed Ring-Opening Carbonyl-Olefin Metathesis. *Organic Letters*. **20**, 4954-4958 (2018).
22. Albright, H. et al. Catalytic Carbonyl-Olefin Metathesis of Aliphatic Ketones: Iron(III) Homo-Dimers as Lewis Acidic Superlectrophiles. *Journal of the American Chemical Society*. **141**, 1690-1700 (2019).
23. Tran, U. P. N., Oss, G., Pace, D. P., Ho, J., Nguyen, T. V. Tropylium-Promoted Carbonyl-Olefin Metathesis Reactions. *Chemical Science*. **9**, 5145-5151 (2018).
24. Tran, U. P. N. et al. Carbonyl-Olefin Metathesis Catalyzed by Molecular Iodine. *ACS Catalysis*. **9**, 912-919 (2019).
25. Catti, L., Tiefenbacher, K. Brønsted Acid-Catalyzed Carbonyl-Olefin Metathesis inside a Self-Assembled Supramolecular Host. *Angewandte Chemie International Edition*. **57**, 14589-14592 (2018).
26. Greenwood, N. N. The Ionic Properties and Thermochemistry of Addition Compounds of Gallium Trichloride and Tribromide. *Journal of Inorganic and Nuclear Chemistry*. **8**, 234-240 (1958).

27. Greenwood, N. N., Perkins, P. G. 68. Thermochemistry of the Systems which Boron Trichloride and Gallium Trichloride Form with Acetone and Acetyl Chloride, and the Heat of Solution of Boron Tribromide in Acetone. *Journal of the Chemical Society Resumed*. 356 (1960).
28. Ludwig, J. R. et al. Mechanistic Investigations of the Iron(III)-Catalyzed Carbonyl-Olefin Metathesis Reaction. *Journal of the American Chemical Society*. **139**, 10832-10842 (2017).
29. Djurovic, A. et. al. Synthesis of Medium-Sized Carbocycles by Gallium-Catalyzed Tandem Carbonyl-Olefin Metathesis/Transfer Hydrogenation. *Organic Letters*. **21**, 8132-8137 (2019).